Lowry, O. H., Rosebrough, N. J., Farr, A. J., and Randall, R. J. (1951), *J. Biol. Chem. 193,* 265–275.
Maurer, H. R., and Chalkley, G. R. (1967), *J. Mol. Biol. 27,* 431–441.
Olins, A. L., and Olins, D. E. (1974), *Science 183,* 330–332.
Oster, G. (1948), *Chem. Rev. 43,* 319–365.
Rill, R., and Van Holde, K. E. (1973), *J. Biol. Chem. 248,* 1080–1083.
Schachman, H. K. (1959), Ultracentrifugation in Biochemistry, New York, N.Y., and London, Academic Press.
Senior M. B., Olins, A. L., and Olins, D. E. (1975), *Science 187,* 173–175.
Shih, T. Y., and Fasman, G D. (1970), *J. Mol. Biol. 52,* 125–128.
Tuan, D. Y. H., and Bonner, J. (1969), *J. Mol. Biol. 45,* 59–76.
Van Holde, K. E., Sahasrabuddhe, C., Shaw, B. R., Van Bruggen, E. F. J., and Arnberg, A. (1974), *Biochem. Biophys. Res. Commun. 60,* 1365–1370.

Near-Ultraviolet Tyrosyl Circular Dichroism of Pig Insulin Monomers, Dimers, and Hexamers. Dipole–Dipole Coupling Calculations in the Monopole Approximation†

E. Hardin Strickland and Dan Mercola*,‡

ABSTRACT: The tyrosyl circular dichroism (CD) has been calculated using the conformation of pig insulin observed in rhombohedral crystals containing 2 zinc atoms per hexamer. These calculations predict that the tyrosyl CD at 275 nm will be enhanced disproportionally as monomers interact to form dimers and as dimers interact to form hexamers. This enhanced tyrosyl CD ($\Delta\epsilon$ per 5800 molecular weight) results from new coupling interactions generated in the regions of contact between monomers and between dimers. These calculations illustrate that a large CD enhancement may accompany aggregation even in the absence of a conformation change in either monomer. The tyrosyl CD intensities calculated for monomers, dimers, and hexamers of 2-zinc pig insulin are compatible with the experimentally observed CD spectra which are enhanced about fourfold in the hexamer compared with the monomer. Zinc ions and other metals do not contribute directly to the tyrosyl CD but only influence the optical properties by promoting the hexameric state. The relation of the integrity of the molecule to dimer formation and the biological activity of the molecules are discussed. The largest calculated contributions to tyrosyl CD arise from interactions with far-ultraviolet transitions of neighboring aromatic groups. In the hexamer, about half of the tyrosyl CD intensity is calculated to arise from Tyr-A14.

Insulin has several advantages as a model system for a theoretical study of the circular dichroism (CD)[1] arising from tyrosyl side chains. Insulin contains a high proportion of tyrosine (4 mol/mol) and phenylalanine (3 mol/mol) but no tryptophan (Dayhoff, 1975). Detailed x-ray analyses have been carried out on insulin crystals containing either of two or four zinc atoms per hexamer (Blundell et al., 1971, 1972; Hodgkin and Mercola, 1972; Bentley et al., 1976). These studies have revealed that the tyrosyl side chains are distributed over three surfaces of the molecule. One of these surfaces is involved in the formation of the dimer and a second surface is involved in contacts between dimers. The dimer contacts are repeated by the crystallographic threefold symmetry to produce a hexamer of insulin. Each aggregation state of insulin as seen in the crystal structure involves tyrosyl side chains in close contact with neighboring molecules (Figure 1). Therefore, the insulin structure provides several possibilities for comparing the calculated and observed states.

The aggregation properties of insulin in solution have been studied extensively (for reviews, cf. Hodgkin and Mercola, 1972; Blundell et al., 1972). The process is best known for zinc-free insulin at pH 2.0 (Jeffrey and Coates, 1966) and at pH 8.0 (Goldman and Carpenter, 1974). In each case the weight-average, molecular weight has been determined as a function of concentration. A least-squares analysis of the data at each pH value has shown that the scheme, 6 monomers $\rightleftharpoons$ 3 dimers $\rightleftharpoons$ 1 hexamer, best explains the data and agrees completely with the organization found in various crystal forms of insulin (Hodgkin and Mercola, 1972; Blundell et al., 1972). The distribution of species in solution can be manipulated by the addition of zinc or other divalent cations (cf. Hodgkin and Mercola, 1972; Blundell et al., 1972; Goldman and Carpenter, 1974). Under neutral and moderately alkaline conditions, zinc added in amounts of 2 g-atoms per 6 mol of insulin is bound

† From the Laboratory of Nuclear Medicine and Radiation Biology, University of California, Los Angeles, California 90024 (E.H.S.), and the Laboratory of Molecular Biophysics, Department of Zoology, Oxford University, Oxford, England (D.A.M.). *Received December 31, 1975.* This work was supported by Contract AT(04-1) GEN-12 between the Atomic Energy Commission and the University of California, by National Science Foundation Grant GB-43450 (E.H.S.), and by The Royal Society, United Kingdom (D.A.M.).

‡ Present address: Department of Zoology, University of Oxford, Oxford 0X1 3PS, England.

[1] Abbreviations used are: CD, circular dichroism; $\Delta\epsilon$ for left circularly polarized light minus that for right circularly polarized light; r_{min}, minimum separation between monopoles of two different side chains; r_{21}, center-to-center distance separating ring groups; uv, ultraviolet; Tris, tris(hydroxymethyl)aminomethane. The insulin residues are labeled by chain (A or B), position, and, where appropriate, by monomer structure (I or II).

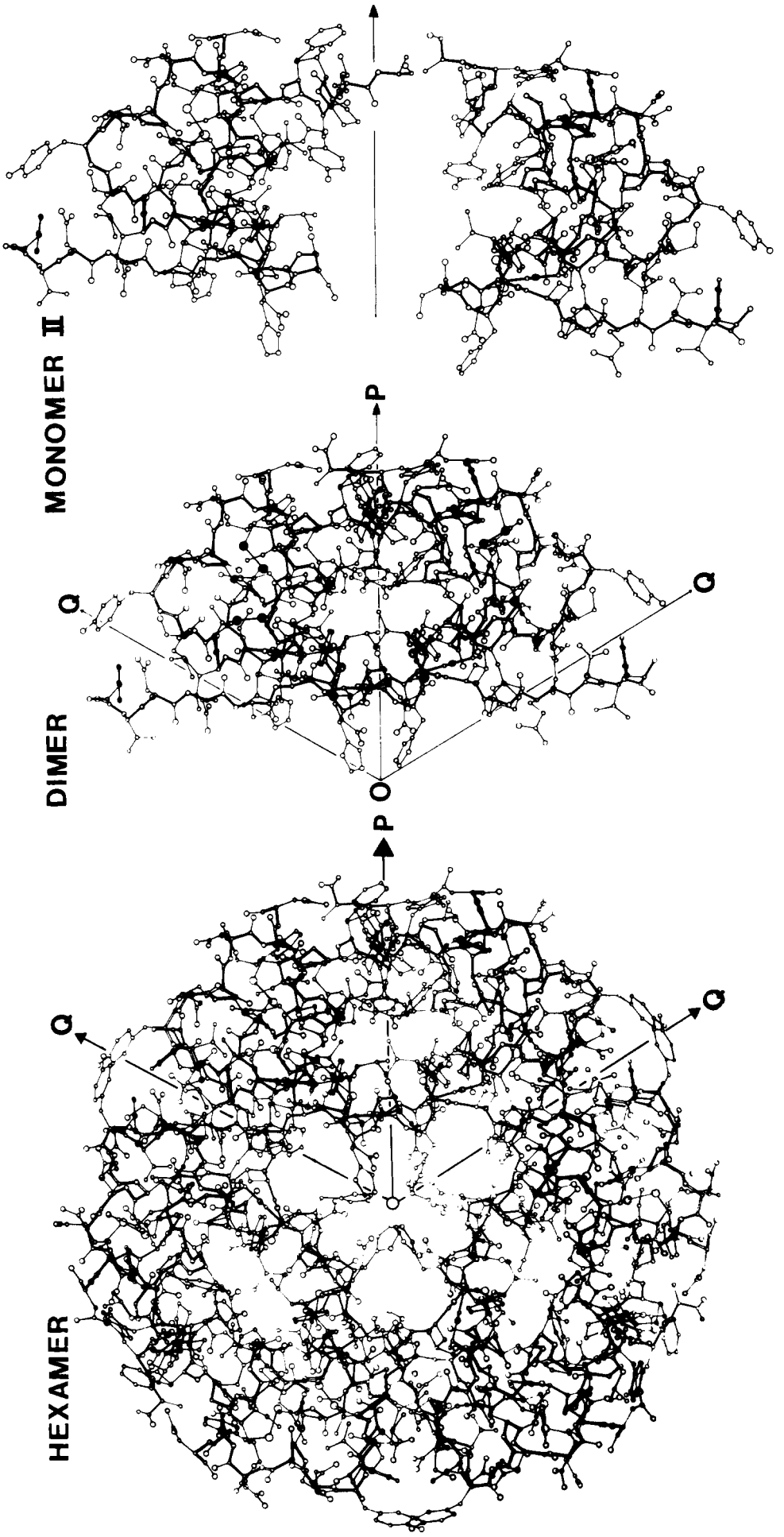

FIGURE 1: Projection down the threefold crystallographic axis of the hexamer showing the development of dimers from the two different monomers and the organization of the dimers in the hexamer.

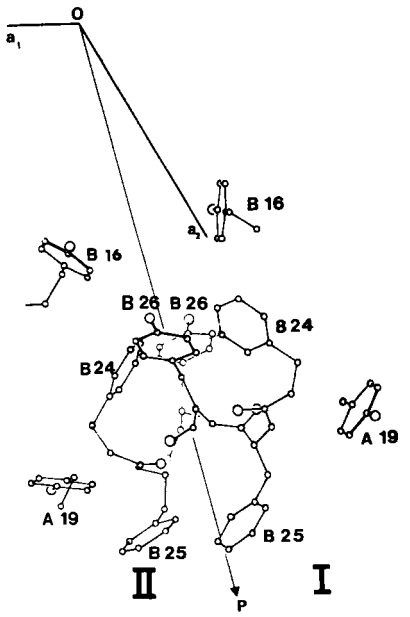

FIGURE 2: A view down the threefold axis showing the residues involved in contacts about the approximate twofold axis (OP) of the dimer. Note the nonequivalent positions of the two Phe-B25.

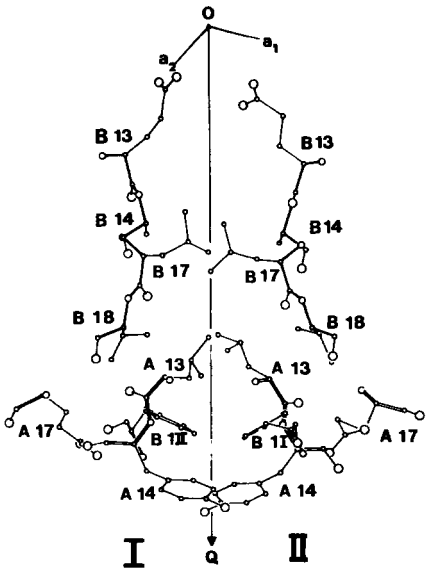

FIGURE 3: A view down the threefold axis of the residues involved in contacts between dimers about the approximate twofold axis (OQ) relating dimers. The two Phe-B1 rings are viewed nearly edge on. Note that the Phe-B1 residues appear on opposite sides of the twofold from the molecule of origin due to the overlap of N-terminal B-chain residues in the hexamer (cf. Figure 1).

almost quantitatively (cf. Hodgkin and Mercola, 1972; Blundell et al., 1972; Pekar and Frank, 1972; Goldman and Carpenter, 1974) and, indeed, leads to hexamer formation (Fredericq, 1953, 1956).

The relationship of chain folding of insulin in solution to that in the crystal structure has been studied by a variety of methods (Arquilla et al., 1969; Mercola et al., 1972), and the data have been reviewed recently (Hodgkin and Mercola, 1972; Blundell et al., 1972). It is reasonably certain that the structure of the zinc-containing hexamer in solution is the same as that found in 2-zinc rhombohedral crystals. Within the hexamer the basic repeating unit is the dimer (Figure 1). The two monomers of the dimer are related by an approximate twofold axis of symmetry (OP) perpendicular to the crystallographic threefold axis, i.e., the two monomer structures are very similar but not identical (Figure 2). In the crystals most aspects of chain folding appear to be relatively well stabilized even in the monomeric and dimeric units. This and other evidence suggests that, for the most part, the molecular conformations of monomers and dimers are probably preserved in solution (Mercola et al., 1972; Blundell et al., 1972).

If conformation differences do exist between the crystalline and solution states of monomers and dimers, the first five residues of the B chain are likely to be involved. When the crystalline hexamer is dissociated (Figure 1), these residues are exposed and less well stabilized than the rest of the structure (Hodgkin and Mercola, 1972). Furthermore, alternative arrangements of this segment even occur in crystals containing 4 zinc atoms per hexamer (Bentley et al., 1976). In the 4-zinc rhombohedral crystals the first eight residues of the N terminus in molecule one undergo a transition from an extended chain to a helix. The transition disrupts contacts between the two N-terminal B chains across the axis OQ (Figure 3). As a result the first seven residues of the B chain of monomer two are also rearranged. The Phe-B1II ring is now packed more compactly against the monomer surface than in the 2-zinc crystals. Therefore, this arrangement must be considered as a possible alternate in solutions of monomers or dimers. In any case, the N terminus of B chain has been found to be fairly rigid in solutions near neutrality even in completely monomeric populations of insulin (Mercola et al., 1972). The chain folding found in molecule II in either the 2- or 4-zinc crystal structures is consistent with present evidence about the structure in solution (Mercola et al., 1972).

In principle, near-ultraviolet CD spectra could provide some information about the orientation of aromatic side chains of insulin in solution. Experimental CD studies have shown that the near-ultraviolet CD intensity per mole is altered greatly by the aggregation state of insulin (Morris et al., 1968; Goldman and Carpenter, 1974). The hexamer CD intensity is most negative and the monomer CD intensity is least negative (Goldman and Carpenter, 1974). Tyrosyl side chains are reported to dominate the CD observed for insulin at 275 nm (Morris et al., 1968; Menendez and Herskovitts, 1970; Ettinger and Timasheff, 1971; Wood et al., 1975). The disulfide bridges probably also make some contribution to the insulin CD at 275 nm, but the exact proportions of tyrosyl and disulfide CD are difficult to determine experimentally (Sears and Beychok, 1973).

Theoretical calculations of the near-ultraviolet CD spectrum of insulin should facilitate understanding the experimental CD spectra. At present only partial calculations are feasible. Apparently reliable calculations of disulfide CD bands have not yet been made for molecules as complex as proteins, although Woody (1973) and Nagarajan and Woody (1973) recently used a method that may be extended eventually in proteins. Tyrosyl CD bands are more easily calculated. In many proteins the tyrosyl CD may be expected to result mainly from electric dipole–electric dipole (μ–μ) coupling (Strickland, 1974). For example, in ribonuclease S, the tyrosyl CD seems to result mainly from the μ–μ coupling interaction between a pair of juxtaposed tyrosyl residues (Strickland, 1972). The tyrosyl CD due to μ–μ coupling may be calculated using either a distributed monopole or a dipole approximation to obtain the interaction energies. Chen and Woody (1971) have pointed out the advantages of calculating the interaction energies from the distributed monopole approximation. A comparison of these

two approximations is possible for insulin. Wollmer and Fleischhaurer (personal communication) have calculated the tyrosyl CD of insulin using the dipole approximation, whereas we have used the other approximation.

In this communication, we describe theoretical calculations of the near-ultraviolet tyrosyl CD bands of insulin based upon the 1.5-Å structure of rhombohedral 2-zinc pig insulin. The calculated results were used to examine several questions about the conformation of insulin in solution. First, do the large CD intensifications observed experimentally after dimer and hexamer formation imply that the conformation of the monomeric units is altered as a result of these interactions? Secondly, are the CD calculations for the structures of insulin monomers in the 2-zinc crystals consistent with the CD spectra observed experimentally? Third, are there any single interactions that contribute a large fraction of the total CD intensity? Finally, do these calculations suggest a way to distinguish experimentally whether one of the two monomers predominates in solution? We are extending these studies to calculations for 4-zinc rhombohedral crystalline insulin and to a comparison of the results obtained with the dipole and distributed monopole approximations for 2- and 4-zinc insulin (Fleischhaurer, Mercola, Strickland, and Wollmer, manuscript in preparation).

Methods

The tyrosyl CD due to μ–μ coupling was calculated as described previously (Strickland, 1972). The interactions between the near-ultraviolet tyrosyl transition and transitions in other groups were considered pairwise, using the monopole approximation to obtain the interaction energies. We treated interactions between the near-ultraviolet tyrosyl transition and the far-ultraviolet π–π^* transitions of the following moieties:[2] the aromatic side chains of Phe(3), His(2), and all other Tyr(3); the amide groups of the peptide backbone(49) and of side chains of Gln(3) and Asn(2); the carboxylate groups(6); and the guanidino group of arginine(1). The rotatory strengths for the interactions between any two groups were the summation of the individual interactions of the near-uv tyrosyl transition in one residue with each of the far-uv transitions in the second group. These rotatory strengths were converted to $\Delta\epsilon$ values at 275 nm, by using the empirical relationship for tyrosyl CD at room temperature:

$$\Delta\epsilon_{275} \doteq 0.5 \times R_s \times 10^{40}$$

All $\Delta\epsilon$ values are expressed per mole of insulin (mol wt 5800), except in tables showing the sum of CD for both molecule one and molecule two.

Degenerate exciton μ–μ couplings between near-uv transitions on two tyrosyl side chains were also calculated, as described previously (Strickland, 1972). For the most part, these interactions would not be measurable contributions to the CD spectra calculated for insulin and, therefore, are not reported here.

Of the calculations reported in this paper, those involving histidinyl and argininyl side chains are of unknown reliability since the spectral properties of these side chains are not well characterized experimentally. Fortunately, the single guanidino group is not close to any tyrosyl side chains in either monomer of insulin, which precludes either guanidino making any significant contribution to the tyrosyl CD.

[2] Numbers in parentheses refer to the number of residues per monomer of insulin.

Initial CD calculations were based on atomic coordinates derived from a 2.8-Å isomorphously phased map of 2-zinc insulin after refinement by alternate cycles of real space refinement and model building procedures as previously described (Blundell et al., 1971). The results reported here are based on atomic coordinates derived from 1.9-Å isomorphously phased map (Blundell et al., 1972; Cutfield, J., Dodson, E., Dodson, G., Hodgkin, D., and Mercola D., manuscript in preparation) which have been refined by model building according to a series of difference Fourier syntheses using as coefficients

$$|F_o - F_c| \exp(-2\pi i \alpha_c)$$

where F_o and F_c are the observed and calculated structure amplitudes, respectively, for planes extending to 1.5-Å spacing and α_c are the corresponding calculated phases based on the current model. The "R" value, $\Sigma|F_o - F_c|/\Sigma|F_c|$, calculated from the coordinates used here for all reflections in the 1.5-Å sphere is 37.6%. The two data sets of coordinates gave significantly different $\Delta\epsilon$ values for some interactions, even though the total CD was not much affected by the refinement. These differences serve to emphasize the need for highly accurate atomic coordinates in order to make reliable CD calculations.

Results

The total tyrosyl CD intensities calculated for the various aggregation states are summarized in Table I. For the monomers the tyrosyl CD intensity is weakly negative. It becomes increasingly negative as the monomers interact to form dimers and the dimers interact to form hexamers. Even though the conformations of the insulin molecules are assumed to be unaffected by aggregation, the CD intensity increases due to the additional interactions that occur. This process can be understood by considering in more detail the interactions occurring within each insulin molecule and between molecules of the aggregates.

For the monomer the CD intensity is only about -0.5 M^{-1} cm^{-1} in each case, although the causes of this weakness differ. In monomer one, none of the interactions are especially strong, whereas in monomer two the CD is weakened by cancellation of oppositely signed contributions (Table I).

The CD arising from Tyr-A14 coupling with the ring of Phe-B1 illustrates an important point. The A14 and B1 rings of each monomer are in van der Waals contact, but their geometry differs somewhat in the two monomers. In monomer one no CD results from Tyr-A14 coupling with the Phe-B1 ring (Table II). Interaction of these same groups in monomer two generates an impressively intense negative CD (-1.4 M^{-1} cm^{-1} in Table III). Thus small differences in the geometry of Tyr-A14 and Phe-B1 can cause large differences in the CD calculated for their interaction.

Interestingly, large differences in geometry do not necessarily have much affect on the CD intensity. A major difference between monomer one and monomer two is the position of Phe-B25. In monomer two the Phe-B25 ring is close by the Tyr-A19 ring (r_{21} = 5.3 Å), whereas in monomer one these rings are much further apart (r_{21} = 9.6 Å). Neither interaction, however, gives much CD intensity (Tables II and III).

Turning now to the dimer, we shall examine the additional interactions occurring when two monomers are brought together. There are two hydrophobic faces on the monomer. One face contains the interaction between Tyr-A14 and Phe-B1 phenylalanine, while the second, more extended face is on the opposite side of the molecule (Figure 1) and contains Tyr-B16, Phe-B24, Phe-B25, and Tyr-B26 (Figure 2). The dimer is

TABLE I: Calculated CD Intensities of Tyrosyl Side Chains of 2-Zn Insulin Conformations.

Insulin Species	$\Delta\epsilon_{275}$ (M^{-1} cm^{-1})			
	Tyr-Tyr or Phe[b]	Tyr-PB[a]	Tyr-Amide	Total[c]
Monomer				
Monomer one	−0.39	−0.50	0.50	−0.4 ± 0.5
Monomer two	−1.53	0.23	0.81	−0.5 ± 0.5
				Total: −0.9 ± 1.0
Dimer				
Monomer one	−1.42	−1.32	0.48	−2.3 ± 0.5
Monomer two	−1.64	−1.09	0.84	−1.9 ± 0.5
				Total: −4.2 ± 1.0
Dimer in hexamer environment				
Monomer one	−2.29	−1.13	0.63	−2.8 ± 0.6
Monomer two	−4.15	−0.67	0.90	−3.9 ± 0.8
				Total: −6.7 ± 1.4

[a] PB, peptide bond chromophore. [b] The remaining possible ring interaction, Tyr-His, was found to yield no CD for all possible Tyr-His combinations. [c] Uncertainty in calculated total is estimated to be at least ±0.5 M^{-1} cm^{-1} or ±20%, whichever is larger.

formed by the interactions between two of these larger surfaces. There are 111 contacts of less than 4-Å separation between the two molecules. Some of these contacts originate in a stretch of antiparallel β structure formed between the monomers across the OP axis. This entire region is very congested which leads, in part, to violations of exact symmetry. This effect is especially noticeable in the positions of the two Phe-B25 ring groups which are in van der Waals contact (Figure 2). Dimerization leads to several other close associations among the eight ring groups in this region (Table III).

Tyrosyl near-ultraviolet CD calculated for the dimer is −3 M^{-1} cm^{-1} more than that obtained by adding the CD of the two monomers in the noninteractive condition (Table I). The additional CD results mainly from interacting between the rings of Tyr-B16 and Tyr-B26 on the two molecules and the interactions between these tyrosyls and several peptide bonds on the neighboring molecule (Table IV). In general interactions between two rings may induce near-ultraviolet CD in either or both rings as a result of the nondegenerate coupling[3] (Strickland, 1972). Tyr-B16I and Tyr-B26II interact to give a major CD contribution (−1.0 M^{-1} cm^{-1}). Almost all of this CD belongs to the near-ultraviolet band of Tyr-B26II, as a result of its coupling with the far-ultraviolet transitions on the ring of Tyr-B16I. In contrast, the interactions between Tyr-B16II and Tyr-B26I effectively cancel each other. The near-ultraviolet band of Tyr-B26I is −0.66 as a result of these interactions.

Several interactions between tyrosyl rings and juxtaposed peptide bonds contribute significantly to the CD enhancement upon dimer formation; e.g., Tyr-B16I and peptide bond B8II, −0.65; Tyr-B16II and peptide bond B7I, −0.40; Tyr-B26II and peptide bond B20I, −0.36 (Table IV). The strength of these interactions arises partly because the ring of each Tyr-B16 is packed against the B-chain helix of the neighboring molecule. For dimer formation the CD intensification due to interactions between tyrosyls and peptide bonds (−2.1) is almost twice as large as that due to interactions between aromatic rings (−1.1).

When the dimer is located in a hexamer environment, additional contacts occur between dimers across the axis OQ (Figure 3). Threefold repetition of these contacts leads to the hexamer (Figure 1). The contacts between dimers only involve four aromatic groups. The A14 tyrosyl groups of neighboring dimers approach each other closely and are bonded through a distorted hydrogen bond between phenolic hydroxyl functions. Two nondegenerate interactions between the two pairs of Tyr-A14 rings give a major CD contribution[4] (total of −1.0, Table V). Each of these interactions contributes nearly equally to the total (−0.4 and −0.59). The close association of the Phe-B1 and Tyr-A14 rings within the monomer structures leads to additional intermolecular contacts between the Tyr and Phe rings in the hexamer (Figure 3). The interaction between Tyr-A14II and Phe-B1I in the dimer is calculated to yield a major tyrosyl CD contribution (−1.6, Table V). However, the corresponding interaction between Tyr-A14I and Phe-B1II in the dimer does not give any measurable CD (Table V). This difference is due to the lack of symmetry relating the Phe-B1 rings and was noticed previously in the CD calculations for the two monomers (see above).

Since the additional interactions giving major CD are all negative, the CD calculated for the dimer in a hexamer environment is much more negative than that calculated for the isolated dimer (Table I). This increased tyrosyl CD (−2.5 for the dimer) is determined almost entirely by the ring–ring interactions among the four groups shown in Figure 3. No other residues approach the A14 tyrosyls, because they are near the surface of the hexamer and also because they are isolated from the rest of the structure by the B1 phenylalanyl rings.

Another aspect of the tyrosyl CD deserves emphasis. When

[3] In addition to the nondegenerate tyrosyl CD bands, two degenerate exciton interactions occur between near-ultraviolet CD bands on neighboring tyrosyls: Tyr B16I-Tyr B26II and Tyr B16II-Tyr B26I. The CD spectra calculated for both of these exciton pairs have about the same intensities, but their spectra have opposite CD signs at each wavelength. Thus, these exciton interactions effectively cancel each other.

[4] The degenerate exciton interactions are calculated to have some influence on the shape of the near-ultraviolet CD spectrum, but the effect does not appear measurable at room temperature. The two pairs of interactions involving Tyr-A14 both give exciton spectra whose longest wavelength band (Strickland et al., 1972) is positive. By cooling to 77 K, the exciton effects might become large enough to be observed as a small distortion of the shape of the CD spectrum. At 77 K the longest wavelength band of the exciton CD spectrum has a calculated $\Delta\epsilon$ value of about 1.2 M^{-1} cm^{-1} (total for both pairs of interactions).

TABLE II: Insulin Molecule One as Monomer.[a]

μ_1 (Near Uv)	μ_2 (Far Uv)	r_{min}[b] (Å)	$\Delta\epsilon_{275}$ (M^{-1} cm^{-1})
Tyr-A14	Phe-B1	2.6	0.00
	PB-A12	3.5	0.27
	PB-A13	2.3	−0.22
	PB-A14	4.8	−0.08
	PB-B1	4.9	0.09
	Glu-A17	4.4	0.09
			Total: 0.15
Tyr-A19	Tyr-B26	6.1	−0.52
	Phe-B24	6.2	0.14
	Phe-B25	5.9	0.27
	PB-A1	4.6	−0.10
	PB-A2	4.9	−0.05
	PB-A5	8.3	0.09
	PB-A15	4.1	0.05
	PB-A16	3.3	−0.18
	PB-A17	3.4	0.19
	PB-A18	1.8	−0.22
	PB-A19	4.2	0.17
	PB-B25	3.0	−0.12
	PB-B26	4.5	0.21
	PB-B27	4.6	0.24
	Asn-A18	3.6	0.23
	Glu-A4	7.6	−0.01
			Total: 0.39
Tyr-B16	Phe-B24	4.6	0.03
	PB-B12	5.0	0.14
	PB-B13	4.6	0.07
	PB-B15	4.5	0.00
	PB-B16	1.9	−0.08
	PB-B17	4.6	−0.26
	PB-B19	4.1	0.00
	PB-B20	2.6	−0.37
	Glu-B13	7.0	0.02
			Total: −0.45
Tyr-B26	Tyr-A19	6.1	−0.16
	Phe-B24	4.7	0.20
	Phe-B25	7.5	−0.09
	His-B5	12.2	0
	PB-A3	5.7	0.25
	PB-B8	4.1	−0.23
	PB-B10	5.7	−0.22
	PB-B11	3.4	−0.01
	PB-B25	3.6	0.04
	PB-B26	2.0	0.46
	PB-B27	2.9	−0.17
			Total: 0.07
			Total for monomer I: 0.16

[a] Moieties having either strong μ–μ coupling or small separations from the Tyr side chain. [b] r_{min} is the shortest separation between monopoles of interacting groups. These monopoles are located in the orbitals above and below the nuclear plane of each group (Strickland, 1972).

TABLE III: Insulin Molecule Two as Monomer.[a]

μ_1 (Near Uv)	μ_2 (Far Uv)	r_{min}[b] (Å)	$\Delta\epsilon_{275}$ (M^{-1} cm^{-1})
Tyr-A14	Phe-B1	2.2	−1.42
	PB-A12	3.6	0.26
	PB-A13	2.9	−0.19
	PB-A14	4.5	0.04
	Glu-A17	4.9	−0.11
			Total: −1.42
Tyr-A19	Tyr-B26	6.0	−0.38
	Phe-B24	6.3	0.13
	Phe-B25	2.2	−0.27
	PB-A1	3.7	−0.24
	PB-A2	4.4	−0.21
	PB-A5	6.1	0.18
	PB-A15	2.8	0.07
	PB-A16	2.8	−0.16
	PB-A17	2.8	0.31
	PB-A18	1.5	−0.30
	PB-A19	4.4	0.20
	PB-B25	3.5	−0.15
	PB-B26	4.6	0.27
	PB-B27	4.9	0.13
	Gln-A5	3.7	0.23
	Asn-A18	3.7	0.37
			Total: 0.18
Tyr-B16	Phe-B24	4.7	0.00
	PB-B13	4.4	0.00
	PB-B14	5.2	−0.13
	PB-B15	4.1	0.03
	PB-B16	1.3	0.22
	PB-B17	4.2	−0.29
	PB-B19	4.5	0.01
	PB-B20	4.6	−0.30
			Total: −0.46
Tyr-B26	Tyr-A19	6.0	0.04
	Phe-B24	5.2	0.35
	Phe-B25	6.2	0.28
	PB-A2	4.6	−0.02
	PB-B8	4.3	−0.05
	PB-B10	5.9	−0.19
	PB-B11	3.8	0.00
	PB-B25	4.4	0.06
	PB-B26	2.1	0.44
	PB-B27	2.7	0.01
	PB-B28	5.2	0.29
			Total: 1.21
			Total for monomer II: −0.49

[a] Moieties having either strong μ–μ coupling or small separation from the Tyr side chain. [b] r_{min} is the shortest separation between monopoles of interacting groups.

the dimer is in a hexamer environment, Tyr-A14II contributes more than half of the total tyrosyl CD intensity of −6.7 (Table I). Most of the CD calculated for Tyr-A14II arises from two interactions: Tyr-A14II with Phe-B1II in the monomer (−1.4, Table III) and Tyr-A14II with Phe-B1I in the hexamer (−1.6, Table V).

As a final point regarding the CD of 2-zinc insulin, we examine briefly the disulfide bridges of insulin. The dihedral angles of the bonds have changed appreciably as the x-ray data had been refined. At the time of calculations described here (R = 37.6%, see Methods and Materials), four of the disulfide bridges in the dimer have dihedral angles near 90° and two of the bridges give the values near −60° (Table VI). For dihedral angles of −60°, one would expect the disulfide bonds to have strong inherent optical activity with the longest wavelength CD band having a negative sign. For dihedral angles near 90°, the inherent CD is expected to be weak (Ludescher and Schwyzer, 1971; Woody, 1973; Sears and Beychok, 1973). Although the total disulfide CD is dependent upon both the induced and inherent optical activity (Woody, 1973; Sears and Beychok, 1973), the values for the dihedral angles do suggest that the disulfide bridges probably give a nonzero contribution to the near-ultraviolet CD of insulin.

TABLE IV: Additional Interactions Occurring as a Result of Dimer Formation.[a]

μ_1 (Near Uv)	μ_2 (Far Uv)	r_{min}[b] (Å)	$\Delta\epsilon_{275}$ (M^{-1} cm^{-1})
Tyr-B16I	Tyr-B26II	2.9	−0.02
	His-B10II	6.8	0.16
	PB-B7II	4.3	−0.23
	PB-B8II	2.0	−0.65
	PB-B9II	4.6	0.18
	PB-B10II	5.5	−0.23
	PB-B11II	5.0	0.13
			Total: −0.66
Tyr-B26I	Tyr-B16II	2.7	−0.66
	Phe-B24II	2.6	−0.17
	PB-B15II	4.8	0.00
	PB-B19II	4.9	−0.02
	PB-B20II	3.5	0.13
	PB-B21II	4.6	−0.03
	PB-B22II	4.5	−0.16
	PB-B23II	3.7	−0.03
			Total: −0.94
Tyr-B16II	Tyr-B26I	2.7	0.70
	His-B5I	11.7	0.00
	His-B10I	6.6	0.10
	PB-B4I	13.2	0.00
	PB-B5I	10.5	−0.06
	PB-B6I	7.4	0.00
	PB-B7I	4.5	−0.40
	PB-B8I	2.0	−0.31
	PB-B9I	3.8	0.06
	PB-B10I	5.3	−0.25
	PB-B11I	4.9	0.10
			Total: −0.06
Tyr-B26II	Tyr-B16I	2.9	−0.98
	Phe-B24I	2.4	0.30
	PB-B12I	6.2	−0.12
	PB-B15I	5.2	0.04
	PB-B16I	5.9	0.17
	PB-B20I	3.7	−0.36
	PB-B21I	4.9	0.00
	PB-B22I	4.4	−0.21
	PB-B23I	4.2	0.07
	PB-B24I	5.0	−0.04
			Total: −1.13
			Total for dimer: −2.79

[a] Moieties having either strong μ–μ coupling or a small separation from the Tyr side chains. [b] r_{min} is the shortest separation between monopoles of interacting groups.

Discussion

The CD spectra of proteins lacking tryptophan are often relatively simple to interpret. For example, the near-ultraviolet CD bands of ribonuclease (Horwitz et al., 1970; Horwitz and Strickland, 1971) and of ovomucoid (Kay et al., 1974) may be resolved approximately into tyrosyl, phenylalanyl, and disulfide contributions, based upon a few experimental techniques. Interpreting the experimental CD spectra of insulin, however, is more complex owing to the monomer–dimer–hexamer equilibria. Unfortunately, in many CD studies of insulin the aggregation state has not been specified. Consequently, an appendix has been included to interpret and summarize data on the experimental CD values for insulin monomers, dimers, and hexamers at 275 nm. The experimental $\Delta\epsilon$ value per 5800 molecular weight increases dramatically as the aggregation proceeds (Table VII). The CD intensity *per monomer* is enhanced about fourfold in the hexamer relative to the monomer!

For each aggregation state, one needs to know which moieties contribute to the near-ultraviolet CD maximum. Since phenylalanyl side chains give only CD bands located below 270 nm (Strickland, 1974), they will not be discussed here. The relative contributions of tyrosyl and cystinyl side chains to the CD may sometimes be estimated from either the wavelength profile or chemical modifications of selected side chains (Strickland, 1974). For hexameric insulin, these approaches suggest both a negative tyrosyl and a negative disulfide contribution to the CD at 275 nm (data reviewed by Sears and Beychok, 1973). To provide an approximate reference point, we note that a crude wavelength profile analysis suggests that the tyrosyls contribute from 50 to 85% of the insulin CD at 275 nm in the hexamer.

The tyrosyls may give proportionally less of the insulin CD in the dimer and monomer. Two experimental observations tend to support this possibility. First, the tyrosyl shoulder at 283 nm seems to become less prominent in CD spectra when the hexamer is dissociated, e.g., Figure 4 in Goldman and Carpenter (1974) and Figure 1 in Morris et al. (1968). Secondly, dissociating the hexamer shifts the CD maximum from 275 nm toward 273 nm (Goldman and Carpenter, 1974). This shift is consistent with a larger proportion of the insulin CD arising from a negative disulfide band with its maximum at 273 nm or below. Apparently the loss of CD intensity upon dissociating the hexamer to dimers and monomers reflects loss of tyrosyl CD.

With these considerations in mind, we shall compare the experimental CD intensities of insulin with the tyrosyl CD intensities calculated for 2-zinc insulin. The calculated tyrosyl CD intensities are less negative than the corresponding experimental values (Table VII). Interestingly, the difference between the experimental $\Delta\epsilon$ value at 275 nm and the calculated tyrosyl $\Delta\epsilon$ values is about -0.8 M^{-1} cm^{-1} for each aggregation state. Perhaps this difference represents the disulfide CD contribution at 275 nm, as the size and wavelength are appropriate for the disulfide CD in a protein (Strickland, 1974). Furthermore, the disulfide bridges of 2-zinc insulin are predicted to have inherent optical activity whose dominant contribution will give negative CD at 275 nm (Table VI).

The comparison between the experimental and calculated CD intensities suggests the following scheme for the CD enhancement accompanying aggregation of insulin. In the monomer about half or more of the CD intensity at 275 nm arises from a negative disulfide band. With each aggregation step, the insulin CD at 275 nm becomes much more negative because the negative tyrosyl CD intensifies. Apparently the disulfide CD intensity may not be affected much by the aggregation process.

This scheme has important implications for interpreting the experimental CD studies on insulin. Our results clearly show that the experimental CD data are consistent with the association scheme proposed on the basis of x-ray studies on 2-zinc insulin crystals (Blundell et al., 1972). Aggregation may occur without any change in conformation of the insulin molecule. The enhanced CD of the hexamer may result entirely from the additional coupling interactions of the tyrosyl rings located in the regions of contact between dimers (Table V) and between monomers (Table IV).

The extent to which our calculations support the proposed scheme depends upon the reliability of our calculated tyrosyl CD intensities. Thus far, our calculations have been tested in only one other protein, ribonuclease S. For ribonuclease S, the

TABLE V: Additional Interactions Occurring When Dimer Is in Hexamer Environment.[a]

μ_1 (Near Uv)	μ_2 (Far Uv)	r_{min}[b] (Å)	$\Delta\epsilon_{275}$ (M^{-1} cm^{-1})
	Interactions with Dimer Rotated +120°	$x_2 = -\frac{1}{2}(x_1 + \sqrt{3}y_1)$ $y_2 = \frac{1}{2}(\sqrt{3}x_1 - y_1)$	
Tyr-A14I	Tyr-A14II	2.6	−0.59
	Phe-B1II	2.4	0.08
	Glu-A17II	6.2	−0.04
			Total: −0.55
Tyr-B16I	Phe-B1II	10.7	−0.15
	His-B10II	5.9	−0.1
	Gln-B4II	3.1	−0.09
			Total: −0.34
	Interactions with Dimer Rotated −120°	$x_2 = -\frac{1}{2}(x_1 - \sqrt{3}y_1)$ $y_2 = -\frac{1}{2}(\sqrt{3}x_1 + y_1)$	
Tyr-A14II	Tyr-A14I	2.5	−0.40
	Phe-B1I	1.5	−1.65
			Total: −2.05
Tyr-B16II	His-B10I	5.4	−0.1
	Gln-B4I	3.5	−0.03
			Total: −0.13
		Total for dimer in hexamer environment:	−3.07

[a] Moieties having either strong μ–μ coupling or a small separation from Tyr side chains. [b] r_{min} is the shortest separation between monopoles of interacting groups.

TABLE VI: Inherent Optical Activity of the Disulfide Bonds of 2-Zinc Insulin.

Cys	Dihedral Angle[a] (deg)	CD of Longest λ Band[a,b] (250–280 nm)
A6I-A11I	92.3	W
A7I-B7I	88.6	W
A20I-B19I	−64.6	−S
A6II-A11II	98.7	W
A7II-B7II	86.5	W
A20II-B19II	−59.1	−S

[a] Measured using the convention and diagram of Ludescher and Schwyzer (1971). [b] W, weak; −S, strong negative CD.

agreement between the experimental and calculated CD spectra is good (Strickland, 1972). Nevertheless, the calculated tyrosyl CD intensities do involve a number of assumptions, which may eventually need to be modified (Strickland, 1972). For example, the tyrosyl side chains may have some mobility. To perform our calculations, we assumed that insulin remains rigid in the three aggregation states. At present, the CD calculations for 2-zinc insulin are easily reconciled with the experimental CD spectra currently available.

As our final point, we describe an interesting relationship between insulin aggregation and the biological activity of the hormone. It has been recognized for some time that the native conformation of the molecule is required for high biological activity (Arquilla et al., 1969; Mercola et al., 1972; Blundell et al., 1972). Similarly, there is growing evidence that the native structure is necessary for the aggregation process. For example, desasn^{A21}-desala^{B30}-insulin has less than 5% biological activity and shows a much reduced ability to form dimers and bind zinc (Goldman and Carpenter, 1974). The zinc-dependent CD of insulin has been investigated in a number of derivatives of insulin that have reduced activity and in several different sequences of insulin with varying biological activity (Goldman and Carpenter, 1974; Wood et al., 1975; A. Wollmer, personal communication). The extent of inactivation of the hormone correlates well with the ability of zinc to promote tyrosyl CD (A. Wollmer, personal communication). Formally, the zinc-dependent CD changes of insulin are complex and could reflect numerous properties such as an aggregation-dependent conformation change as in glucagon (Blanchard and King, 1966). Our calculations, however, show that intermolecular contacts between native insulin molecules are sufficient to explain the aggregation phenomenon without invoking any mechanisms of conformation change. This suggests that the ability of an insulin derivative to aggregate is a measure of the similarity of the conformation of that derivative to the native conformation. The correlation between biological activity and aggregation emphasizes the role of the three-dimensional structure in the mechanisms of action of insulin. In particular it draws attention to the surfaces of the molecule that are involved in intermolecular contacts. The possible role of these surfaces in the mechanism of action has been reviewed recently (Blundell et al., 1972). The results described here are consistent with the view that the integrity of surface involved in dimer formation may be particularly important in generating a biological response.

Acknowledgments

We thank Professor Axel Wollmer and Dr. Guy Dodson for describing their unpublished results and for helpful discussions.

Appendix

Experimental CD Values for Insulin Monomers, Dimers, and Hexamers. The observed $\Delta\epsilon$ value for the hexamer state

TABLE VII: Comparison between Experimental CD of Insulin and Tyrosyl CD Calculated for 2-Zinc Insulin.

	$\Delta\epsilon_{275}$[a]				
Aggregation State	Obsd for Insulin	Ref	Corrected to Single Species[b]	Calcd for Tyr	$(\Delta\epsilon_o - \Delta\epsilon_c)$[c]
Hexamer	−4.2	*d-i*	−4.2	−3.4	−0.8
Dimer	−2.9	*g*	−3.0	−2.1	−0.9
	−3.1	*l*	−3.3[j]		−1.2
Monomer	−1.9	*g, i*	−1.2	I: −0.4	−0.8, −0.3
				II: −0.5	−0.7, −0.2
			−0.7[j]		

[a] Per 5800 molecular weight. [b] Details of correction are given in Appendix. [c] The difference in observed and calculated CD per 5800 molecular weight. Value may represent disulfide CD intensity. [d] Morris et al., 1968. [e] Menendez and Herskovitts, 1970. [f] Ettinger and Timasheff, 1971. [g] Goldman and Carpenter, 1974. [h] Wollmer, personal communication. [i] Wood et al., 1975. [j] Value given by Wood et al., 1975.

in Table I is an average of values obtained under two conditions: (a) zinc added to zinc-free insulin at pH 8.0; and (b) solutions of commercial crystalline insulin dissolved in more neutral solutions. Commercial crystalline insulin generally contains about 0.35% zinc and in neutral solution at concentrations of about 0.25% insulin has a molecular weight of 36 000, which corresponds to the 2-zinc hexamer (Sjögren and Svedberg, 1931; Blundell et al., 1972). The average CD value obtained for several solutions of zinc insulin in the pH range 7.0 to 7.5 (Morris et al., 1968; Menendez and Herskovitts, 1970; Ettinger and Timasheff, 1971) and one study at pH 7.8 ($\Delta\epsilon_M = -4.12$ M^{-1} cm^{-1}, A. Wollmer, personal communication, 1975) is −4.18 M^{-1} cm^{-1}. At pH 8.0 insulin quantitatively binds sufficient zinc to satisfy the 2-zinc hexamer stoichiometry (Goldman and Carpenter, 1974; Wood et al., 1975; A. Wollmer, personal communication, 1975). The average of values at pH 8.0 taken from the range 0.33 to 0.66% zinc is −4.24 M^{-1} cm^{-1}, in good agreement with measurements in the more neutral pH range. The overall average ($n = 7$) is −4.20 M^{-1} cm^{-1} (Table VII).

CD values corresponding to a predominance of dimers or monomers have been obtained by working with zinc-free insulin at pH 8 (Goldman and Carpenter, 1974; Wood et al., 1975). Wood et al. (1975) have used the equilibrium constants determined by Goldman and Carpenter (1974) to estimate the fraction of monomeric (negligible) and hexameric species in equilibrium and, using the $\Delta\epsilon$ for hexamer, have corrected their measured value to that corresponding to a 100% dimer population ($\Delta\epsilon = -3.3$ M^{-1} cm^{-1}, Table VII). When the same procedure is applied to the CD data of Goldman and Carpenter (1974), a similar value ($\Delta\epsilon = -3.1$) is obtained (Table VII). The corrected values are within about 5% of the respective values observed experimentally. This is due to the large proportion of dimers present under the conditions of measurement. These corrections assume that equilibrium constants determined in 0.1 M NaCl (Goldman and Carpenter, 1974) apply to insulin in the solutions used for the CD measurements (water, Goldman and Carpenter, 1974; 0.025 M Tris, Wood et al., 1975). This assumption is probably justified. For example, the monomer–dimer equilibrium constant at pH 7.0 for 0.1 M NaCl with 0.1 M Tris is 1.4×10^5 (Pekar and Frank, 1972), which is similar to the value of 2.2×10^5 obtained at pH 8.0 with only 0.1 M NaCl (Goldman and Carpenter, 1974). The difference in these two constants corresponds to a redistribution of total protein of about 8%.

Much less is known about the circular dichroism of the monomer of insulin, in part due to technical difficulties in obtaining measurements of highly dilute solutions. Measured values of −1.9 M^{-1} cm^{-1} have been reported for two different concentrations: 2.5×10^{-5} M insulin by Goldman and Carpenter (1974) and 3.8×10^{-5} M insulin by Wood et al. (1975). According to the equilibrium constants of Goldman and Carpenter (1974), however, these solutions contain much dimer in addition to the monomer (monomer mole fractions of 0.60 and 0.45, respectively). Therefore, large extrapolations are required to correct these values to those expected for 100% monomer solutions. The corrections for the two observations at pH 8.0 lead to considerably disparate results (Table VII). Two reasons may be involved in these differences. Wood et al. used a somewhat larger value for the corrected dimer molar CD; and, more importantly, their solution contained a higher fraction of dimer.

References

Arquilla, E. R., Bromer, W. W., and Mercola, D. A. (1969), *Diabetes 18,* 193.

Bentley, G., Dodson, E., Dodson, G., Hodgkin, D. C., and Mercola D. A. (1976), *Nature (London) 261,* 166.

Blanchard, M. H., and King, M. V. (1966), *Biochem. Biophys. Res. Commun. 25,* 298.

Blundell, T. L., Cutfield, J. F., Cutfield, S. M., Dodson, E. J., Dodson, G., Hodgkin, D. C., Mercola, D. A., and Vijayan, M. (1971), *Nature (London) 231,* 506.

Blundell, T. L., Dodson, G., Hodgkin, D., and Mercola, D. A. (1972), *Adv. Protein Chem. 26,* 279.

Chen, A. K., and Woody, R. W. (1971), *J. Am. Chem. Soc. 93,* 29.

Dayhoff, M. O. (1975), Atlas of Protein Sequence and Structure, Vol. 5, Washington, D.C., National Biomedical Research Foundation.

Ettinger, M. J., and Timasheff, S. N. (1971), *Biochemistry 10,* 824.

Fredericq, E. (1953), *Nature (London) 171,* 570.

Fredericq, E. (1956), *Arch. Biochem. Biophys. 65,* 218.

Goldman, J., and Carpenter, F. H. (1974), *Biochemistry 13,* 4566.

Hodgkin, D. C., and Mercola, D. A. (1972), in Handbook of Physiology, Section 7, Vol. I, Part I, Geiger, S. R., Ed., Washington, D.C., American Physiological Society, p 139.

Horwitz, J., and Strickland, E. H. (1971), *J. Biol. Chem. 246,* 3749.

Horwitz, J., Strickland, E. H., and Billups, C. (1970), *J. Am. Chem. Soc. 92,* 2119.

Jeffrey, P. D., and Coates, J. H. (1966), *Biochemistry 5,* 3820.

Kay, E., Strickland, E. H., and Billups, C. (1974), *J. Biol. Chem. 249,* 797.

Ludescher, U., and Schwyzer, R. (1971), *Helv. Chim. Acta 54,* 1637.
Menendez, C., and Herskovitts, T. (1970), *Arch. Biochem. Biophys. 140,* 286.
Mercola, D., Morris, J. W. S., and Arquilla, E. R. (1967), *Biochim. Biophys. Acta 133,* 224.
Mercola, D., Morris, J. W. S., and Arquilla, E. R. (1972), *Biochemistry 11,* 3860.
Morris, J. W. S., Mercola, D. A., and Arquilla, E. R. (1968), *Biochim. Biophys. Acta 160,* 145.
Nagarajan, R., and Woody, R. W. (1973), *J. Am. Chem. Soc. 95,* 7212.
Pekar, A. H., and Frank, B. H. (1972), *Biochemistry 11,* 4013.
Sears, D. W., and Beychok, S. (1973), in Physical Principles and Techniques of Protein Chemistry, Part C, Leach, S. J., Ed., New York, N.Y., Academic Press, p 566.
Sjögren, B., and Svedberg, T. (1931), *J. Am. Chem. Soc. 53,* 2657.
Strickland, E. H. (1972), *Biochemistry 11,* 3465.
Strickland, E. H. (1974), *Crit. Rev. Biochem. 2,* 113.
Strickland, E. H., Wilchek, M., Horwitz, J., and Billups, C. (1972), *J. Biol. Chem. 247,* 572.
Wood, S., Blundell, T., Wollmer, A., Lazarus, N., and Neville, R. (1975), *Eur. J. Biochem. 55,* 531.
Woody, R. W. (1973), *Tetrahedron 29,* 1273.

Use of Gel Chromatography for the Determination of the Stokes Radii of Proteins in the Presence and Absence of Detergents. A Reexamination†

Yasuhiko Nozaki, Norman M. Schechter, Jacqueline A. Reynolds, and Charles Tanford*,‡

ABSTRACT: In the course of a routine investigation of the complex between the erythrocyte membrane protein spectrin and sodium dodecyl sulfate, we observed a large discrepancy between the true Stokes radius (178 Å, measured by hydrodynamic methods) and the apparent value derived from gel chromatography (107 Å). In attempting to resolve this discrepancy, we have experiments that indicate that all large asymmetric particles may be subject to a similar discrepancy; e.g., native fibrinogen has a true Stokes radius of 108 Å, whereas the value derived by column chromatography after calibration with globular proteins is only 71 Å. The simplest interpretation is that end-on insertion of asymmetric particles into the gel pores contributes to their retardation. The phenomenon clearly limits the usefulness of gel chromatography as a quantitative measure of the hydrodynamic Stokes radius. Incidental data obtained in the course of this work indicate that spherical viruses may have weak chemical affinity for the porous gel. Chromatography of large proteins in the presence of detergents produced no effects ascribable to adsorption of the detergents, but the results suggest a need for further study of possible interaction between detergents and small gel pores.

The discovery by Porath and Flodin (1959) that cross-linked dextran gels can fractionate water-soluble molecules on the basis of molecular size has had a profound impact on protein chemistry, providing not only a practical tool for purification, but also an analytical tool for the measurement of relative molecular dimensions, and for the study of equilibria in reactions accompanied by a change in dimensions (Ackers, 1970). However, there have been no definitive studies relating the dimensional parameter that determines exclusion from the gel pores to actual physical measures of molecular size. An early proposal (Andrews, 1965) was that relative rates of elution of proteins are uniquely determined by molecular weight, but this holds true (even approximately) only when all proteins being compared belong to the same conformational class, e.g., if all are globular proteins or all are linear random coils (Fish et al., 1969). When proteins of different conformational types have been compared, it has been tacitly assumed that relative rates of elution are governed by the Stokes radius (R_s) of the protein particle. This radius is formally defined in terms of the frictional coefficient, $f \equiv 6\pi\eta R_s$ (where η is the viscosity of the solvent) and can be directly determined from the diffusion coefficient or by simultaneous measurement of molecular weight and sedimentation velocity (Tanford, 1961). The only serious test of this assumption (Laurent and Killander, 1964) is effectively limited to globular proteins with R_s at 60 Å or below. Warshaw and Ackers (1971) showed that the assumption is in fact false even for this class of proteins when elution characteristics are measured with high precision, but their work has had little impact because gel chromatography is usually used in circumstances where approximate answers (±10%) suffice. Work from this laboratory (Fish et al., 1970; Tanford et al., 1974) has indicated that the assumption is valid within a 10% uncertainty in the range of R_s = 30–80 Å. The comparisons in the latter studies involved proteins in three different conformational states: globular proteins in aqueous solution, random coils in guanidine hydrochloride, and complexes between proteins and sodium dodecyl sulfate. An additional conclusion implicit in the results was thus that drastic alterations in the solvent medium (including the presence of detergents) do not significantly alter the pore size distribution and elution characteristics of the chromatographic columns.

The reinvestigation of this problem described in this paper was prompted by discrepancies between observed and expected

† From the Department of Biochemistry, Duke University Medical Center, Durham, North Carolina 27710. *Received February 13, 1976.* This work was supported by research Grants BMS 73-01328 from the National Science Foundation and AM-04576 from the National Institutes of Health.

‡ Research Career Awardee, National Institutes of Health.